Synthesis of unsymmetrical monocarbonyl curcumin analogues with potent inhibition on prostaglandin E_2 production in LPS-induced murine and human macrophages cell lines

Mohd Fadhlizil Fasihi Mohd Aluwi, Kamal Rullah, Bohari M. Yamin, Leong Sze Wei, Mohd Nazri Abdul Bahari, Lim Sock Jin, Siti Munirah Mohd Faudzi, Juriyati Jalil, Faridah Abas, Norsyahida Mohd Fauzi, Nor Hadiani Ismail, Ibrahim Jantan, Lam Kok Wai

PII: S0960-894X(16)30324-9
DOI: http://dx.doi.org/10.1016/j.bmcl.2016.03.092
Reference: BMCL 23735

To appear in: *Bioorganic & Medicinal Chemistry Letters*

Received Date: 16 December 2015
Revised Date: 21 January 2016
Accepted Date: 25 March 2016

Please cite this article as: Aluwi, M.F.F., Rullah, K., Yamin, B.M., Wei, L.S., Bahari, M.N.A., Jin, L.S., Faudzi, S.M.M., Jalil, J., Abas, F., Fauzi, N.M., Ismail, N.H., Jantan, I., Wai, L.K., Synthesis of unsymmetrical monocarbonyl curcumin analogues with potent inhibition on prostaglandin E_2 production in LPS-induced murine and human macrophages cell lines, *Bioorganic & Medicinal Chemistry Letters* (2016), doi: http://dx.doi.org/10.1016/j.bmcl.2016.03.092

Graphical Abstract

Synthesis of unsymmetrical monocarbonyl curcumin analogues with potent inhibition on prostaglandin E_2 production in LPS-induced murine and human macrophages cell lines

Mohd Fadhlizil Fasihi Mohd Aluwi[a] , Kamal Rullah[a] , Bohari M. Yamin[d] , Leong Sze Wei[b] , Mohd Nazri Abdul Bahari[b] , Lim Sock Jin[a] , Siti Munirah Mohd Faudzi[b, e] , Juriyati Jalil[a] , Faridah Abas[b] , Norsyahida Mohd Fauzi[a] , Nor Hadiani Ismail[c] , Ibrahim Jantan[a] , Lam Kok Wai[a, *]

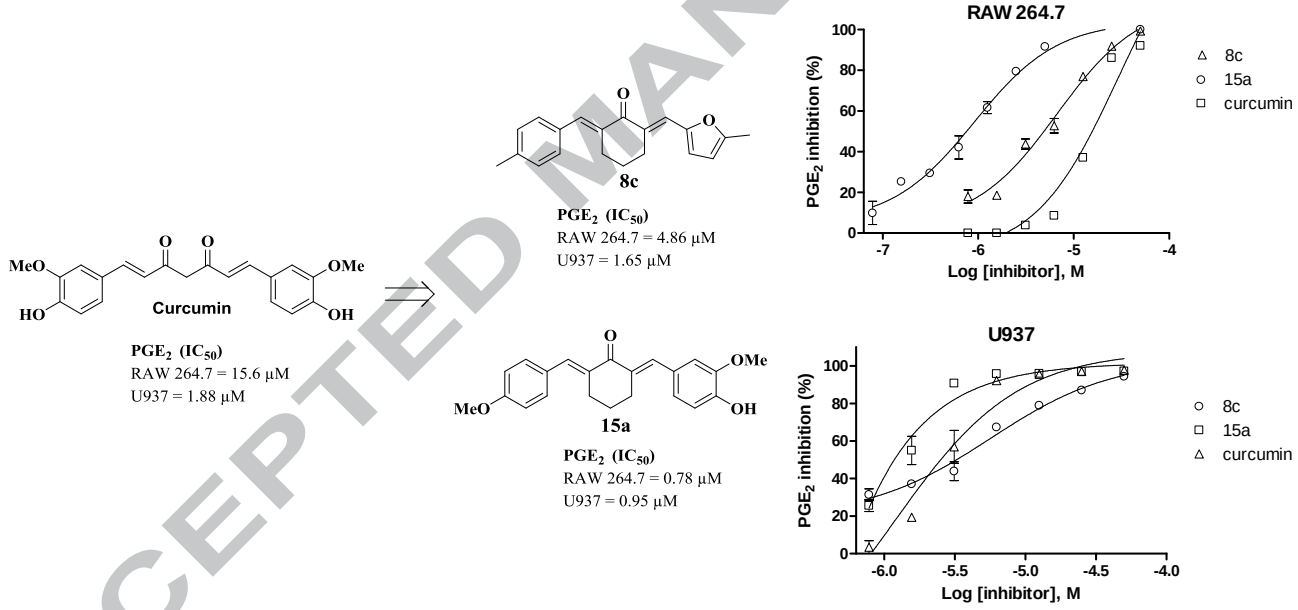

Bioorganic & Medicinal Chemistry Letters
journal homepage: www.elsevier.com

Synthesis of unsymmetrical monocarbonyl curcumin analogues with potent inhibition on prostaglandin E_2 production in LPS-induced murine and human macrophages cell lines

Mohd Fadhlizil Fasihi Mohd Aluwi[a], Kamal Rullah[a], Bohari M. Yamin[d], Leong Sze Wei[b], Mohd Nazri Abdul Bahari[b], Lim Sock Jin[a], Siti Munirah Mohd Faudzi[b,e], Juriyati Jalil[a], Faridah Abas[b], Norsyahida Mohd Fauzi[a], Nor Hadiani Ismail[c], Ibrahim Jantan[a], Lam Kok Wai[a,*]

[a]*Drug and Herbal Research Centre, Faculty of Pharmacy, Universiti Kebangsaan Malaysia, Jalan Raja Muda Abdul Aziz, 50300, Kuala Lumpur, Malaysia*
[b]*Laboratory of Natural Product, Institute of Bioscience, Universiti Putra Malaysia, 43400, Serdang, Selangor, Malaysia*
[c]*Atta-Ur- Rahman Institute for Natural Product Discovery, Universiti Teknologi MARA Kampus Puncak Alam, 42300, Puncak Alam, Selangor, Malaysia*
[d]*School of Chemical Sciences and Technology, Universiti Kebangsaan Malaysia, 43600, Bangi, Selangor, Malaysia*
[e]*Department of Chemistry, Faculty of Science, Universiti Putra Malaysia, 43400, Serdang, Selangor, Malaysia*

ARTICLE INFO

Article history:
Received
Revised
Accepted
Available online

Keywords:
Unsymmetrical curcumin analogues
Prostaglandin E_2
RAW264.7
U937
Single-crystal XRD
Cyclooxygenase-2

ABSTRACT

The syntheses and bioactivities of symmetrical curcumin and its analogues have been the subject of interest by many medicinal chemists and pharmacologists over the years. To improve our understanding, we have synthesized a series of unsymmetrical monocarbonyl curcumin analogues and evaluated their effects on prostaglandin E_2 production in lipopolysaccharide-induced RAW264.7 and U937 cells. Initially, compounds **8b** and **8c** exhibited strong inhibition on the production of PGE_2 in both LPS-stimulated RAW264.7 (**8b**, IC_{50} = 12.01 µM and **8c**, IC_{50} = 4.86 µM) and U937 (**8b**, IC_{50} = 3.44 µM and **8c**, IC_{50} = 1.65 µM) cells. Placing vanillin at position Ar_2 further improved the potency when both compounds **15a** and **15b** significantly lowered the PGE_2 secretion level (RAW264.7: **15a**, IC_{50} = 0.78 µM and **15b**, IC_{50} = 1.9 µM while U937: **15a**, IC_{50} = 0.95 µM and **15b**, IC_{50} = 0.92 µM). Further experiment showed that compounds **8b**, **8c**, **15a** and **15b** did not target the activity of downstream inflammatory COX-2 mediator. Finally, docking simulation on protein targets COX-2, IKK-β, ERK, JNK2, p38α and p38β were performed using the conformation of **15a** determined by single-crystal XRD.

The production of prostaglandin E_2 (PGE_2) can be triggered by the event of infection or inflammation. It is known that accumulation of excessive PGE_2 in the body could lead to various diseases such as cancer, rheumatoid arthritis, atherosclerosis and pain. The biosynthesis of PGE_2 is initiated from the stimulus-induced liberation of arachidonic acid (AA) from membrane phospholipids by the phospholipase A_2 (PLA_2) enzyme. AA is then sequentially metabolized into prostaglandin G_2 and further converted to prostaglandin H_2 (PGH_2) by either cyclooxygenase-1 (COX-1) or cyclooxygenase-2 (COX-2). Finally, the unstable intermediate PGH_2 can be catalyzed by any of the three forms of prostaglandin synthase (PGES), namely mPGES-1, mPGES-2, and cPGES, [1-3] to form the bioactive lipid prostaglandin E_2 (PGE_2) (Figure 1).

Curcumin is the main active ingredient isolated from *Curcuma longa* L. also referred to as diarylheptanoid. Previous studies showed that consumption of curcumin is extremely safe even at very high doses in various animal models [4] or human studies [5]. Nevertheless, curcumin has been shown to exhibit great chemical and pharmacological potential as antioxidant, anti-proliferation, anti-angiogenesis, anti-tumour and anti-inflammation [6-10]. It has also been investigated for COX inhibitory activity using the bovine seminal vesicles, microsomes and cytosol from homogenates of mouse epidermis with reported IC_{50} values of 2 µM, 52 µM and 5–10 µM, respectively [11-13]. Despite that, accumulating evidence suggests that curcumin is highly unstable and has a poor bioavailability when tested *in vitro* and *in vivo*. Some of the efforts to improve the stability of curcumin have been made recently including replacing the β-diketone moiety of the curcumin structure with a cyclohexanone or 4-piperidone ring [14-17].

Previously, our group has established the synthesis of symmetrical curcumin analogues and evaluated their effects on a

* Corresponding author. Tel.: +60 3 9289 7031
E-mail: david_lam@ukm.edu.my

variety of biological activities including anti-inflammatory, anti-tyrosinase and immunomodulatory [18-21]. The anticancer properties of these curcumin analogues have also been intensively studied by others [22-24]. Based on the recent reports, there were suggestions that the unsymmetrical form of demethoxycurcumin derivative (Figure 2) might possess greater biological profile compared to the symmetrical form of bisdemethoxcurcumin [25, 26]. This was further supported by our work on the synthesis of unsymmetrical diarylpentadione **1** [27], diarylpentadienone **2** [28] and 2-benzoyl-6-benzylidinecyclohexanone **3** [17] which were found to actively repress the NO production in RAW 264.7 cells (Figure 2). In our continuing effort to search for new anti-inflammatory agents with higher efficacy and better safety profiles, we have synthesized a series of new unsymmetrical monoketone diarylpentanoid analogues and evaluated their effects on PGE_2 production against the lipopolysaccharide-induced murine RAW 264.7 and human U937 macrophages cell lines. The active compounds were further tested on the ability to inhibit human COX-2 activity.

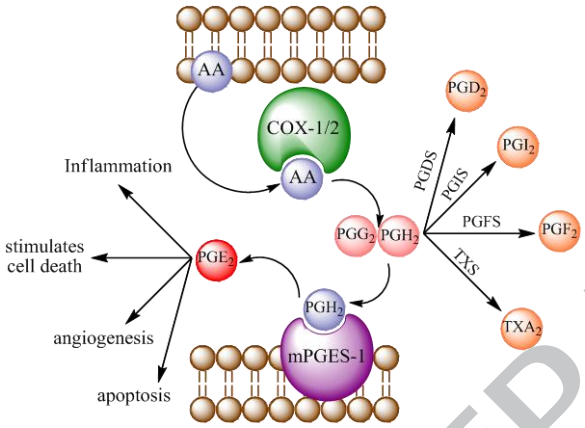

Figure 1. Biosynthesis of PGE_2 from arachidonic acid by COX-1/2 and mPGES-1.

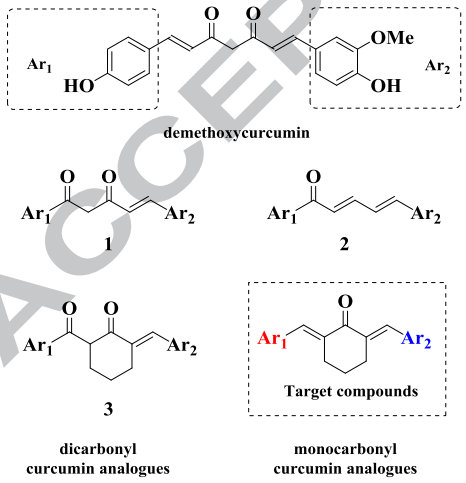

Figure 2. Naturally isolated unsymmetrical demethoxycurcumin, synthetic unsymmetrical dicarbonyl, and monocarbonyl curcumin analogues.

The syntheses of monocarbonyl curcumin analogues **8a-e**, **12a-d** and **15a-e** were accomplished by steps outlined in Scheme 1. Initially, mono-benzylidene cyclohexanone, **6** was prepared by simple aldol condensation reaction using pyrolidine as catalyst in ethanol solvent as reported by Chimni and co-workers (2005) [29]. The singlet peak at 7.58 ppm with integration of one found in the ^{1}H NMR spectra confirmed the presence of olefinic proton in the half aldol condensation product of **6** (Fig.S-1, Supplementary Data). Crude product **6** was coupled with respective benzaldehydes, **7** in the presence of NaOH at room temperature to furnish the desired unsymmetrical monocarbonyl curcumin analogues **8a-e** in satisfactory yields. To initiate the synthesis of compounds **12a-d**, Suzuki-Miyaura coupling reaction was employed utilizing the carbon-carbon single bond formation between 4-bromobenzaldehyde, **9** and 4-fluroboronic acid, **10** to afford 4-fluorophenylbenzaldehyde, **11** and reacted with **6** using the Claisen-Schmidt condensation reaction to afford **12a-d**. On the other hand, we have also attempted to replace the cyclohexanone linker with 4-piperidone ring. Several strategies have been employed including masking the reactive amine group of 4-piperidone with *tert*-butyloxycarbonyl and methyl iodide and preparing the mono-benzylidenepiperidone using Mukaiyama aldol reaction as shown in Scheme S-1, Supplementary Data. However, all attempts failed to yield the target unsymmetrical products. Finally, all ^{1}H, ^{13}C NMR and ESI-HRMS spectra were consistent with the assigned structure of the synthesized compounds [30] (Fig. S-2, Fig. S-3 & Fig. S-4, Supplementary Data).

Among compounds **8a-e** tested for their effects on PGE_2 production in LPS/IFN-γ-induced RAW264.7 cells, **8c** appeared to be the frontrunner with excellent inhibition at the screening concentration. Further testing showed that compound **8c** exhibited an IC_{50} of 4.86 µM (Table 1). From the MTT assay, it is clearly shown that the inhibition was not affected by cell viability as it did not fall in close proximity to the tested concentration. Therefore, it can be concluded that the reduction of PGE_2 secretion level was not due to cell death. It is also noteworthy that this compound showed approximately 3-fold higher inhibition than curcumin. Structurally, compound **8c** comprises a five-membered furanyl ring at Ar_2 position could be the key reason that contributes to the activity. This result coincides with the previous report, in which compound containing furanyl ring also exhibited a significant PGE_2 reduction *in vitro* [31] and was further supported that the presence of five-membered heterocyclic ring system is essential for PGE_2 inhibition *in vivo* [32]. Besides, compound **8b** bearing an adjacent pair of dimethoxyl groups at Ar_2 position also displayed a remarkable reduction in the PGE_2 level at the screening concentration with IC_{50} of 12.01 µM. Moreover, compounds containing more than one methoxyl group also enhanced the PGE_2 inhibitory activity *in vitro* [33].

Following the positive results obtained, we next addressed the question of whether the inhibitory action of **8a-e** on PGE_2 production was restricted to murine cells. Therefore, the study was repeated using the human U937 macrophage cell line as it mimics the human *in vivo* condition sharing many characteristics of monocytes and is easy to use [34]. Even though murine cells are the experimental tool of choice for majority pharmacologists and have yielded tremendous results in the past, undeniably both murine and human share significant differences in signaling pathways and protein structures due to genetic and evolution factors. For example, the mPGES-1 inhibitor, MF63 did not show any effects on rat possibly due to difference in substitutions of amino acid residues Thr131, Leu135 and Ala138 (human amino acid sequence) with bulky aromatic residues. It was suggested that these residues occlude the entrance to the active site and therefore prevent some inhibitors from binding [35]. To initiate the experiment, U937 monocyte was first induced with phorbol 12-myristate 13-acetate (PMA) to start to adhere culture plate and differentiate into macrophages. The detail of assay procedure is

explained in the experimental section. Overall, the results were found comparable to the study conducted using RAW264.7 macrophage (Table 2). Compounds **8b** and **8c** bearing the dimethoxyl groups and furanyl ring were again able to reduce the PGE_2 secretion level in the cells while compounds **8a**, **8d** and **8e** only managed to exhibit moderate inhibition. It is assumed that these compounds could interact in a relatively similar mechanistic pathway that is shared between the two species. All active compounds showed non-cyctotoxic profile against the U937 human macrophages at the tested concentration indicate that these compounds may be safe to be implemented in future *in vivo* murine model. Figure S-6 depicts the dose-dependent manner of **8b** and **8c** towards the secretion of PGE_2 with IC_{50} values of 3.44 µM and 1.65 µM (Fig. S-6, Supplementary Data). In contrast, the presence of 2-napthyl, 3, 4-dichlorophenyl and 4-fluorophenylbenzaldehyde in compounds **8a**, **8e** and **12a-d** were not favorable possibly due to their poor solubility in the buffer solution (Table 1).

Previous studies conducted on the symmetrical **BHMC** (Fig. S-1, Supplementary Data) showed that it exhibited potent anti-inflammatory activity in both *in vitro* and *in vivo* [20, 36]. To compare the effects between the symmetrical and unsymmetrical form of demethoxycurcumin derivatives on PGE_2 formation in both macrophages, compounds **15a-e** were designed and synthesized by coupling the THP vanillin moiety **14** with different benzaldehydes, **6** in the presence of base. Subsequently, the THP protecting group was cleaved with *p*-toluene sulfonic acid to afford compounds **15a-e** in satisfactory yield (Scheme 1). As expected, treatment of LPS-induced murine and human macrophages with these compounds strongly suppressed the PGE_2 formation with over 85% inhibition at 25 µM concentration. In both cell lines, compounds **15a** and **15b** displayed even higher potency than curcumin. Figure 3 depicts the dose-dependent graphs of compounds **15a** on the inhibition of PGE_2 and the cytotoxicity against RAW264.7 and U937 cells. From this finding, it is important to note that the presence of a single vanillin moiety at Ar_2 was sufficient to replicate the activity of curcumin. This remarkable observation could serve as important information for the future design of anti-inflammatory inhibitors.

Additionally, the synthesized compounds were tested on the nitric oxide (NO) inhibition using RAW264.7 cell line at 25 µM concentration. Unfortunately, we could not evaluate the NO activity in U937 human macrophages cells due to the reason that the cells did not produce measurable amount of nitrite following induction [18]. Most of the compounds exhibited moderate to strong inhibition except for **12a-d** (Table S-1, Supplementary Data). However, at 25 µM, compounds **8e** and **15a-e** were cytotoxic and therefore it is important to reduce the concentration in the next study.

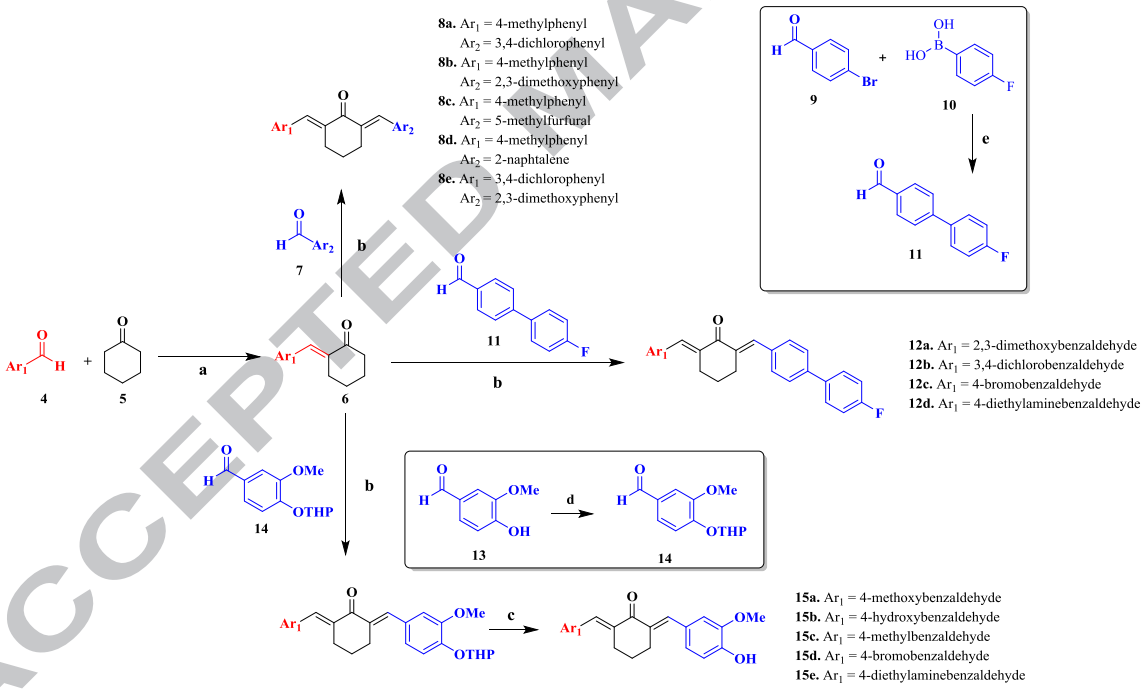

Scheme 1. Reagents and conditions: a) pyrolidine, EtOH, r.t.; b) NaOH, EtOH, r.t.; c) *p*-toluene sulfonic acid, EtOH, r.t.; d) 3,4-dihydro-2*H*-pyran, pyridinium 4-toluenesulfonate, DCM, r.t.; e) HCl (g), AcOH, r.t.

Since compounds **8b**, **8c**, **15a** and **15b** displayed similar inhibitory profiles on the PGE_2 secretion level in the two cell lines, we predicted that these compounds might potentially inhibit the activity of COX-2 enzyme. The reason is simple as COX-2 in both species share common conserved sequence and are structurally homology similar [37]. To determine the selectivity of the compounds on COX isoforms, experiments were conducted using the ovine COX-1 and human recombinant COX-2 ELISA kits and the results were compared with the COX inhibitor, indomethacin which acts as a positive control. At 25 µM concentration, compounds **8b**, **8c**, **15a** and **15b** selectively inhibited COX-2 over COX-1 (Table 2) even though this result did not justify their strong PGE_2 inhibition profile in the cells. Initial docking simulations revealed that compounds **8b**, **8c**, **15a** and **15b** did not interact with Arg513 (Supplementary Data), whereas this residue is known to be a crucial requirement for the time dependent inhibition of COX-2. This implies that the compounds might work on a different protein target or signaling pathway.

It is known that the accuracy of docking result is highly dependent on the initial conformation of the input ligand. Therefore, two crystals of compounds **15a** and **15c** were grown by slowly evaporation from hexane: ethyl acetate (7:3) and were

subjected to single crystal X-ray structural investigation. Both compounds **15a** and **15c** crystallized in monoclinic system with space group a = 15.464(2) Å, b = 8.0410(11) Å, c = 15.537(2) Å, α= 90°, β= 112.431, γ = 90°, Z=4, V=1785.96(17) Å and a=10.0643(10) Å, b=10.5045(10) Å, c=17.2687(16) Å, α=90°, β=94.629(3)°, γ=90°, Z=4, V= 1819.7(3) Å, respectively. It was difficult to get a quality crystal of **15a** despite several attempts of crystallization. However, the data was solved under monoclinic system although the unit cell is unusual. No sign of twinning and pseudo symmetry was detected by PLATON software.

The crystal system and refinement parameters are shown in Table 3. Figure 4 shows the molecular structure with numbering scheme for both compounds. Both compounds display the bird-like molecules consist of a central cyclohexanone ring, (C8-C13)/O1 with its wings of 3-hydroxy-4-methoxybenzylidine (C14-C20)/C22//O2/O3 and *p*-methylbenzylidene, (C1-C7)/C21 groups in **15c** whereas in **15a** the right wing 4-methylbenzylidene is replaced by *p*-methoxybenzylidene, (C1-C7)/O2/C21.

Table 1

In vitro PGE_2 production inhibitory activity of synthesized compounds in LPS/IFN-γ-induced RAW264.7 and U937 cells

Compound	Percentage (%) of PGE_2 inhibition at 25 µM		Percentage (%) of cell viability at 25 µM		IC_{50} (µM)	
	RAW 264.7[a]	U937[b]	RAW 264.7[a]	U937[b]	RAW 264.7[a]	U937[b]
8a	64	68	95	100	n.t	n.t
8b	83	83	100	100	12.01	3.44
8c	92	84	83	98	4.86	1.65
8d	74	66	100	94	n.t	n.t
8e	73	58	77	100	n.t	n.t
12a	51	68	90	98	n.t	n.t
12b	59	76	100	94	n.t	n.t
12c	53	66	92	98	n.t	n.t
12d	65	72	94	100	n.t	n.t
15a	96	86	<50	100	0.78	0.95
15b	96	88	<50	100	1.9	0.92
15c	95	85	<50	100	n.t	n.t
15d	96	87	<50	100	n.t	n.t
15e	95	85	<50	100	n.t	n.t
Curcumin	78	94	90	95	15.95	1.88
Nimesulide[*]	66	89	100	100	<0.078	<0.078

n.t = not tested

[*]Concentration of positive control (nimesulide) used in the experiment (5 µM).

[a] LPS/IFN-γ-induced murine macrophage cell line.

[b]LPS/IFN-γ-induced human macrophage cell line.

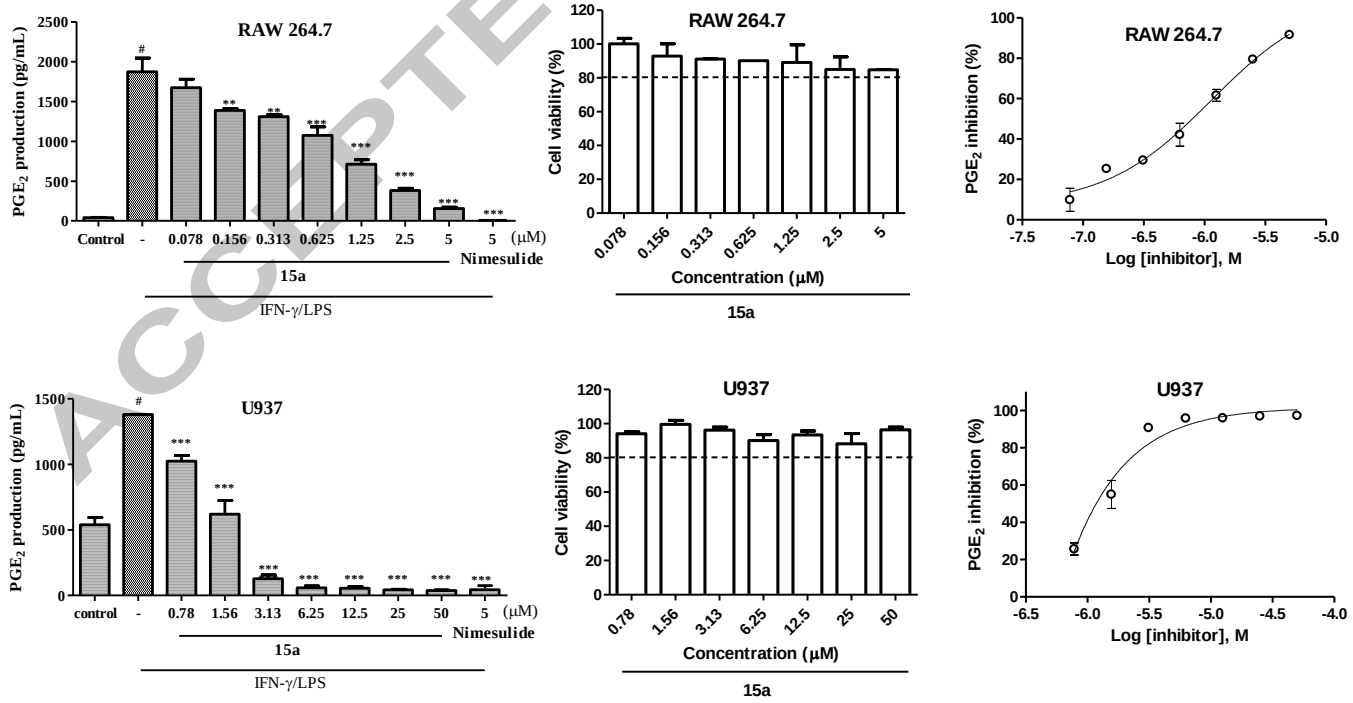

Figure 3. Effects of compound **15a** on PGE_2 production in LPS-stimulated RAW264.and U937 cells. The cells were co-incubated with LPS (2µg/mL) and different concentrations of compounds ranging from 0.78 to 50µM. The supernatants were then collected for the measurement of PGE_2 production. The values are expressed as the means ± SD of three individual samples. P< 0.001 as compared with the LPS-treated macrophages; significant differences between groups were determined using one-way ANOVA test followed by a Dunnett's multiple comparison test. #P< 0.05 solvent control compared with the LPS-treated cells; significant difference was determined using unpaired student's-test (n.s. is not significant).

In compound **15c**, the central cyclohexyl ring (C8-C13) adopts a twisted half chair conformation with maximum deviation of 0.349(3) Å for C12 atom from the least square plane. The bond lengths and angles are in normal ranges (Table S-3) with double bond character of C7-C8 and C10-C14 bonds (1.334(3) and 1.342(3) Å, respectively). Both wings are planar with maximum deviation of 0.049(4) Å for C21 atom of the least square plane of the *p*-methylbenzylidine ring. The dihedral angle between the two wings is 21.64(10)°. The central cyclohexanone makes dihedral angles with the 3-hydroxy-4-methoxybenzylidine (C14-C20)/C22//O2/O3 and *p*-methylbenzylidene, (C1-C7)/C21 of 48.96(11) and 47.35(13)°, respectively. There is a weak O2-H2...O3 intramolecular hydrogen bonds. The structure of the molecule is stabilized by O2-H2...O1 (1/2+x,3/2y,-1/2z, D-A= 2.807(3)Å, D-H-A= 152°) and C7- H7-O2 (-1/2x,3/2-y,1/2+z, D-A=3.570(4)Å , D-H-A= 168°) intermolecular hydrogen bonds. The bonding parameters in the analogous **15a** are very much comparable with those in **15c**. However the dihedral angles between the wings 3-hydroxy-4-methoxybenzylidine (C14-C20)/C22//O3/O4 and *p*-methoxybenzylidene, (C1-C7)/O1/C21 with the central cyclohexanone, (C8-C13) are slightly smaller than those in **15c** of 23.35(11) and 46.43(13)°, respectively. In the crystal structure the molecule is stabilized by O3-H13...O1, C21-H21B...O4 and C22-H22...O2 intermolecular hydrogen bonds. The crystallographic data for the structural analysis were deposited with the Cambridge Crystallographic Data Centre No **1446853 (15a)** and **1441911** (**15c**).

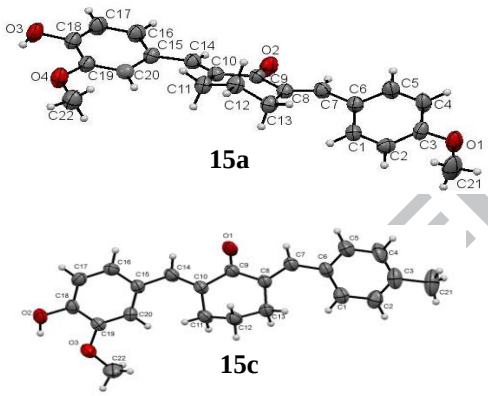

Figure 4. Molecular structure of **15a** and **15c** with numbering scheme drawn at 50% probability ellipsoids.

Since the compounds did not directly suppress PGE_2 production *via* COX-2, we predicted that it might target the transcription factor level. LPS mediated the stimulation of TLR4 and subsequently activating NF-κB and MAPK signaling pathways which have been recognized as one of the crucial transcription factors known to regulate COX-2 expression. Interruptions of these signaling pathways may down-regulated the COX-2 expression, thus reduced the PGE_2 production. It has been reported that the symmetrical monocarbonyl curcumin analogues could interrupt these signaling pathways in both *in vitro* and *in vivo* [22, 38, 39]. Therefore, the obtained crystal XRD of **15a** was employed in docking simulations using protein crystal structures of IKK-*β* (**3RZF**), ERK (**5BVD**), JNK2 (**3NPC**), p38*α* (**1A9U**) and p38*β* (**3GP0**). The cDOCKER interaction energies were used as a measurement to compare the binding affinity of compound **15a** with the co-crystallized ligands (Table 4). Among the target enzymes, compound **15a** showed favorable cDOCKER interaction energy of -38.45 kcal/mol (p38*α*) and -42.63 kcal/mol (IKK-*β*) which closely resembled the cDOCKER interaction energy of their co-crystallized ligands, -40.62 kcal/mol and -42.63 kcal/mol, respectively. In the p38*α* binding site, the vanillin moiety could interact by forming a single hydrogen bond (2.06 Å) with Phe169. Furthermore, the cyclohexanone carbonyl oxygen of **15a** could form a hydrogen bond (2.01 Å) with Lys53 (Figure 5). On the other hand, a strong hydrogen bond could be observed between the oxygen atom of methoxyl moiety of **15a** with Cys99 (2.59 Å) in IKK-*β* binding site (Figure 5). A weak π-π interaction (5.63 Å) between *p*-methoxyphenyl and phenol side chain of Tyr98 could also be observed. Overall, **15a** displayed lower binding affinity in other target enzymes as compared to their co-crystallized ligands. This result is in agreement with the previous report, in which the inhibitory activity of curcumin analogues were more pronounced on p38*α* and IKK-*β* [40, 41]. Thus, it is suggested that **15a** could preferably target p38*α* or IKK-*β*, subsequently down-regulated the COX-2 expression and eventually reduced the PGE_2 production.

Table 2
COX-1 and COX-2 inhibition activity

Compound	Percentage (%) inhibition at 25 µM	
	COX-1	COX-2
8b	n.a	23
8c	n.a	30
15a	n.a	22
15b	n.a	27
Curcumin	n.a	24
Indomethacin	100	100

n.a = not active

Table 3
Crystal and structure refinement parameters of compound **15a** and **15c**

Identification code	15a	15c
Empirical formula	$C_{22}H_{22}O_4$	$C_{22}H_{22}O_3$
Formula weight	350.39	334.39
Temperature	301(2) K	303(2) K
Wavelength	0.71073 Å	0.71073 Å
Crystal system	Monoclinic	Monoclinic
Space group	$P2_1/n$	$P2_1/n$
Unit cell dimensions	a = 15. 464(2) Å b = 8.0410 (11) Å c = 15.5370(2) Å *α*= 90° *β*= 112.431(3)° *γ* = 90°	a = 10.0643(10) Å b = 10.5045(10) Å c = 17.2687(16) Å *α*= 90° *β*= 94.629(3)° *γ* = 90°
Volume	1785.8(4) $Å^3$	1819.7(3) $Å^3$
Z	4	4
Density (calculated)	1.303 Mg/m^3	1.221 Mg/m^3
Absorption coefficient	0.089 mm^{-1}	0.080 mm^{-1}
F(000)	744	712
Crystal size	0.500 × 0.180 × 0.090 mm^3	0.500 × 0.480 × 0.420 mm^3
Theta range for data collection	2.873 to 25.996°	2.983 to 26.498°
Index ranges	-19<=h<=19, -9<=k<=9, -19<=l<=19	-12<=h<=12, -13<=k<=13, -21<=l<=21
Reflections collected	59594	46798
Independent reflections	3508 [R(int) = 0.2810]	3765 [R(int) = 0.0971]
Completeness to theta = 25.242°	99.9 %	99.8 %
Refinement method	Full-matrix least-squares on F^2	Full-matrix least-squares on F^2
Data / restraints / parameters	3508 / 0 / 239	3765 / 0 / 229
Goodness-of-fit on F^2	1.053	1.090
Final R indices [I>2sigma(I)]	*R*1 = 0.0707, wR2 = 0.1085	*R*1 = 0.0616, w*R*2 = 0.1166
R indices (all data)	*R*1 = 0.1692, wR2 = 0.1365	*R*1 = 0.1152, w*R*2 = 0.1443

Extinction coefficient	n/a	n/a
Largest diff. peak and hole	0.171 and -0.166 e.Å^{-3}	0.211 and -0.188 e.Å^{-3}

Table 4
Comparison of cDOCKER interaction energy between **15a** with target enzyme inhibitors

Enzyme	cDOCKER interaction energy (kcal/mol)	
	15a	co-crystallized ligand*
IKK-*β*	-42.63	-45.75
p38*α*	-38.45	-40.62
P38*β*	-45.25	-77.52
ERK2	-46.90	-74.55
JNK2	-39.46	-80.90

*Retrieved from their PDB crystal structure

On the other hand, the ADMET properties of the synthesized compounds were calculated by the standard descriptors protocol implemented in Discovery Studio 3.1 to predict the pharmacokinetic of the compounds when they are administered and pass through the body. The parameters included in the analysis were human intestinal absorption (HIA), plasma-protein binding (PPB), atom based log P (Alog P98), polar surface area (PSA), aqueous solubility, blood brain barrier (BBB) penetration, cytochrome P_{450} 2D6 (CYP2D6) enzyme inhibition and hepatotoxicity. All of the compounds were predicted to be efficiently absorbed in the human intestine. Specifically, compounds **15a**, **15b, 15c** and **15e** bearing the vanillin moiety showed promising logarithm of the molar solubility value of -5.403, -4.913, -5.87, -6.183 and -5.854, respectively. On the other hand, there was no inhibition on cytochrome P_{450} which means that these compounds can readily undergo oxidation and hydroxylation in the first phase of metabolism. All the compounds were predicted to exhibit ≥90% of plasma-protein binding. This result coincides with the metabolites studies of monocarbonyl curcumin analogues reported by Snyder and co-workers which suggested that the protein binding may serve to protect the curcumin analogues from full metabolism *in vivo* while allowing it to exert a pharmacological effect by means of slow drug release [42]. Only compounds **15a** and **15b** were predicted not to exhibit very high BBB. Notably, all compounds displayed non-hepatotoxic profile. The data are summarized in Table 5.

Table 5.
ADMET profile prediction of selected compounds

Compd	ADMET parameter									
	Human Intestinal Absorption			Aqueous Solubility		Blood Brain Barrier (BBB) Penetration		Plasma Protein Binding (PPB)	Cytochrome P_{450} 2D6 (CYP2D6)	Hepatotoxicity
	PSA[a]	ALogP98[b]	Level[c]	Log(Sw)[d]	Level[e]	LogBB[f]	Level[g]	Prediction[h]	Prediction[i]	Prediction[j]
8b	35.160	5.590	0	-6.502	1	1.018	0	1	0	0
8c	29.855	5.164	0	-6.224	1	0.970	0	1	0	0
15a	55.976	4.862	0	-5.403	2	0.463	1	1	0	0
15b	67.861	4.637	0	-4.913	2	0.205	1	1	0	0
15c	47.046	5.365	0	-5.870	2	0.760	0	1	0	0
15d	47.046	5.627	0	-6.183	1	0.841	0	1	0	0
15e	50.398	5.738	0	-5.854	2	0.822	0	1	0	0

[a] Polar surface area (PSA) (>150: very low absorption).
[b] Atom-based log P (Alog P98) (≤ 2.0 or P ≥ 0: very low absorption).
[c] Level of human intestinal absorption prediction; 0 (good), 1 (moderate), 2 (poor), 3 (very poor).
[d] The based [10]logarithm of the molar solubility log (Sw) (25°C, pH = 7.0) (acceptable drug-like compounds: 6 < log(Sw)≤ 0).
[e] Level of aqueous solubility prediction; 0 (extremely low), 1 (very low), 2 (low), 3 (good), 4 (optimal), 5 (too soluble), 6 (warning: molecules with one or more unknown Alog P calculation).
[f] Very high penetrants (log BBP ≥7).
[g] Level blood brain barrier penetration prediction; 0 (very high penetrate), 1 (high), 2 (medium), 3 (low), 4 (undefined).
[h] Prediction Plasma-protein binding (0: <90%; 1≥90%;).
[I] Prediction cytochrome P_{450} 2D6 enzyme inhibition (0: non-inhibitor; 1: inhibitor).
[j] Prediction hepatotoxicity (0: non-toxic; 1: toxic).

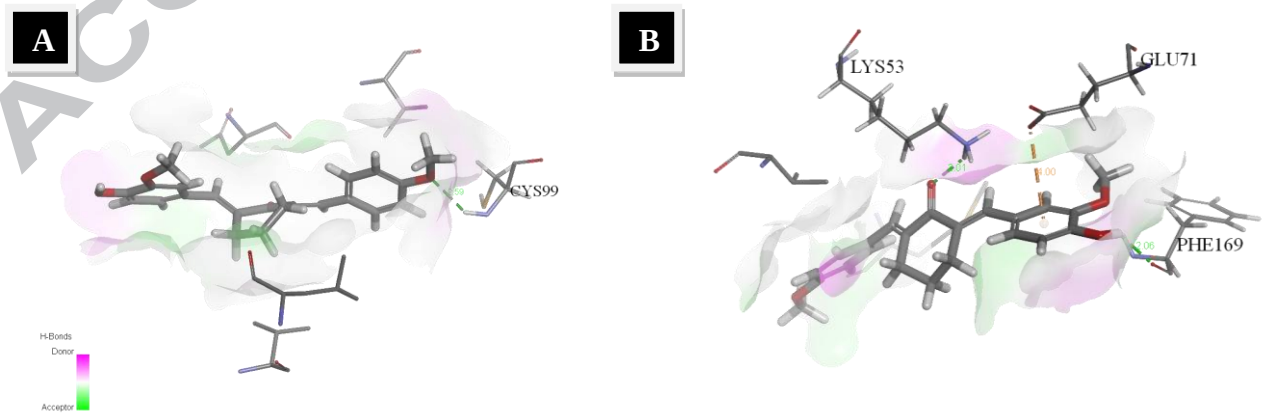

Figure 5. Predicted binding poses retrieved from docking simulation of **15a** in 1KK*β* (**A**) and p38*α* (**B**) putative binding sites. The atom colouring for the compound is in the following: carbons in blue, oxygen in red, nitrogen in blue, and hydrogen in white. The green line indicates hydrogen-bonding interaction while the orange line indicates electrostatic interaction, with distance indicated in angstroms, Å.

In summary, we have successfully determined the effects of unsymmetrical monocarbonyl curcumin analogues on PGE_2 secretion level in LPS-induced murine and human macrophages. Structural features revealed that presence of furanyl ring and vanillin moiety in compounds significantly enhanced the PGE_2 inhibition in both macrophages cells. Detailed binding mode from docking simulations revealed that compounds **8b, 8c, 15a** and **15b** could only form only one hydrogen bond in the COX-2 active site. This fully justifies the reason for their low inhibitory activity in the assay. However, further studies are required to identify the real molecular target(s) and signaling pathway that might contribute to the anti-inflammatory properties of the analogues.

Acknowledgement

This work was financially supported by ScienceFund (02-01-02-SF00665), Ministry of Science, Technology & Innovation, Malaysia and FRGS (FRGS/2/2014/ST01/UKM/02/3), Ministry of High Education, Malaysia. Authors also thank University Kebangsaan Malaysia for the funds provided under the Research University Grant UKM-DIP-2014-16.

References and notes

1. Mbalaviele G., Pauley A.M., Shaffer A.F., Zweifel B.S., Mathialagan S., Mnich S.J., Nemirovskiy O.V., Carter J., Gierse J.K., Wang J.L., Vazquez M.L., Moore W.M., Masferrer J.L., *Biochem. Pharmacol*., **2010**, *79*, 1445.
2. Sampey A., Monrad S., Crofford L., Arthritis Res. Ther., 2005, *7*, 114.
3. Samuelsson B., Morgenstern R., Jakobsson P.-J., *Pharmacol. Rev*, **2007**, *59*, 207.
4. Shankar T.N., Shantha N.V., Ramesh H.P., Murthy I.A., Murthy V.S., , *IJEB*, **1980**, *18*, 73-75.
5. Dhillon N., Aggarwal B.B., Newman R.A., Wolff R.A., Kunnumakkara A.B., Abbruzzese J.L., Ng C.S., Badmaev V., Kurzrock R., *Clin. Cancer Res.*, **2008**, *14*, 4491.
6. Notoya M., Nishimura H., Woo J.-T., Nagai K., Ishihara Y., Hagiwara H., *Eur. J. Pharmaco*, **2006**, *534*, 55.
7. El-Azab M., Hishe H., Moustafa Y., El-Awady E.-S., *Eur. J. Pharmaco.*, **2011**, *652*, 7.
8. Wei X., Senanayake T.H., Bohling A., Vinogradov S.V., *Mol. Pharmaceutics*, **2014**, *11*, 3112.
9. Kant V., Gopal A., Pathak N.N., Kumar P., Tandan S.K., Kumar D., *Int. Immunopharmacol*, **2014**, *20*, 322.
10. Mehta K., Pantazis P., McQueen T., Aggarwal B.B., *Anti-cancer drugs*, **1997**, *8*, 470-481.
11. Ammon H.P.T., Safayhi H., Mack T., Sabieraj J., *J. Ethnopharmacol*, **1993**, *38*, 105.
12. Flynn D.L., Rafferty M.F., Boctor A.M., *Prostaglandins Leukot Med*, **1986**, *22*, 357.
13. Huang M.-T., Lysz T., Ferraro T., Abidi T.F., Laskin J.D., Conney A.H., *Cancer Res.*, 1991, *51*, 813.
14. Liang G., Shao L., Wang Y., Zhao C., Chu Y., Xiao J., Zhao Y., Li X., Yang S., *Bioorg Med Chem*, **2009**, *17*, 2623.
15. Yu P., Dong L., Zhang Y., Chen W., Xu S., Wang Z., Shan X., Zhou J., Liu Z., Liang G., *Eur. J. Med. Chem.*, **2015**, *94*, 436.
16. Zhang Y., Zhao L., Wu J., Jiang X., Dong L., Xu F., Zou P., Dai Y., Shan X., Yang S., Liang G., *Molecules*, **2014**, *19*, 7287.
17. Leong S.W., Mohd Faudzi S.M., Abas F., Mohd Aluwi M.F.F., Rullah K., Lam K.W., Abdul Bahari M.N., Ahmad S., Tham C.L., Shaari K., Lajis N.H., *Bioorg. Med. Chem. Lett.*, **2015**, *25*, 3330.
18. Tham C.L., Liew C.Y., Lam K.W., Mohamad A.-S., Kim M.K., Cheah Y.K., Zakaria Z.-A., Sulaiman M.R., Lajis N.H., Israf D.A., *Eur. J. Pharmacol.*, **2010**, *628*, 247.
19. Lee K.H., Ab. Aziz F.H., Syahida A., Abas F., Shaari K., Israf D.A., Lajis N.H., *Eur. J. Med. Chem*., **2009**, *44*, 3195.
20. Tham C.L., Lam K.W., Rajajendram R., Cheah Y.K., Sulaiman M.R., Lajis N.H., Kim M.K., Israf D.A., *Eur. J. Pharmacol*., 2011, *652*, 136.
21. Bukhari S.N.A., Lauro G., Jantan I., Bifulco G., Amjad M.W., *Bioorg. Med. Chem.*, **2014**, *22*, 4151.
22. Brown A., Shi Q., Moore T.W., Yoon Y., Prussia A., Maddox C., Liotta D.C., Shim H., Snyder J.P., *J. Med. Chem.*, **2013**, *56*, 3456.
23. Thakur A., Manohar S., Velez Gerena C.E., Zayas B., Kumar V., Malhotra S.V., Rawat D.S., *MedChemComm*, **2014**, *5*, 576.
24. Liu Z., Sun Y., Ren L., Huang Y., Cai Y., Weng Q., Shen X., Li X., Liang G., Wang Y., *BMC Cancer*, **2013**, *13*, 494.
25. Sandur S.K., Pandey M.K., Sung B., Ahn K.S., Murakami A., Sethi G., Limtrakul P., Badmaev V., Aggarwal B.B., *Carcinogenesis*, **2007**, *28*, 1765.
26. Yang J.Y., Zhang L.J., Zhao S.Q., Yuan D., Lian G.N., Wang X.X., Zhang H.T., Wang L.H., Wu C.F., *Neurosci. Res.*, **2010**, *68*, 451.
27. Leong S., Faudzi S., Abas F., Aluwi M., Rullah K., Wai L., Bahari M.,. Ahmad S, Tham C., Shaari K., Lajis N., *Molecules*, **2014**, *19*, 16058.
28. Mohd Faudzi S.M., Leong S.W., Abas F., Mohd Aluwi M.F.F., Rullah K., Lam K.W., Ahmad S., Tham C.L., Shaari K., Lajis N.H., *MedChemComm*, **2015**, *6*, 1069.
29. Chimni S.S., Mahajan D., *Tetrahedron*, 2005, *61*, 5019.
30. 1. **(a) Representative synthetic procedures and spectral characterizations**. *General procedure for the preparation of unsymmetrical monocarbonyl curcumin analogues.* Pyrolidine in EtOH (30%, 10mL) was added to a stirred solution of respective benzaldehyde (10 mmol) and cyclohexanone (50 mmol) in absolute EtOH (30mL). The yellowish solution was then subjected to column chromatography with n-hexane/EtOAc (9:1) to afford 2-benzylcyclohexanone. Respective benzaldehyde (10 mmol) was added to a stirred solution of 2-benzylcyclohexanone (10 mmol) in the presence of NaOH (1M) at room temperature. The yellow precipitate obtained was filtered and rinsed with distilled water. The precipitate was purified by flash chromatography with n-hexane/EtOAc (9:1) and recrystallized from absolute ethanol. **(2*E*,6*E*)-2-(2,3-dimethoxybenzylidene)-6-(4-methylbenzylidene) cyclohexanone (8b)**. Yellow amorphous (yield 70%), mp: 130-131°C; ^{1}H NMR (500 MHz, $CDCl_3$) δ 7.79 (d, J = 12.1 Hz, 1H), 7.39 (t, J = 13.1 Hz, 1H), 7.24 (d, J = 8.0 Hz, 1H), 7.14 (dd, J = 8.4, 1.6 Hz, 2H), 7.05 (d, J = 1.6 Hz, 1H), 6.93 (d, J = 8.4 Hz, 1H), 3.95 (s, 1H), 3.94 (s, 1H), 3.15 – 2.92 (m, 114H), 2.41 (s, 2H), 1.83 (dt, J = 12.4, 6.4 Hz, 55H). ^{13}C NMR (126 MHz, $CDCl_3$) δ 190.23, 148.72, 138.77, 136.93, 136.84, 135.51, 134.55, 133.26, 130.83, 130.53, 129.13, 123.96, 113.81, 110.97, 55.95, 28.52, 23.04, 21.38. ESI-HRMS: ($C_{23}H_{24}O_3$) calc. [M+H] 349.1725, found 349.1759. **(2*E*,6*E*)-2-(4-methylbenzylidene)-6-((5-methylfuran-2-yl) methylene)cyclohexanone (8c)**. Brownish crystal (yields 55%), mp: 140-141°C; ^{1}H NMR (500 MHz, $CDCl_3$) δ 7.79 (s, 1H), 7.55 (d, J = 1.9 Hz, 1H), 7.38 (d, J = 8.0 Hz, 2H), 7.23 (d, J = 7.9 Hz, 2H), 6.61 (d, J = 3.2 Hz, 1H), 6.16 (d, J = 3.0 Hz, 1H), 3.00 (t, J = 5.4 Hz, 2H), 2.96 – 2.89 (m, 2H), 1.85 (dt, J = 12.5, 6.3 Hz, 2H). ^{13}C NMR (126 MHz, $CDCl_3$) δ 191.18, 155.55, 151.50, 138.95, 136.33, 135.58, 133.32, 131.53, 130.40, 129.09, 123.94, 117.81, 108.98, 28.29, 28.13, 22.43, 21.38, 14.03. ESI-HRMS: ($C_{20}H_{20}O_2$) calc. [M+H] 293.1463, found 293.1497. **(2*E*,6*E*)-2-(4-methoxybenzylidene)-6-(3-methoxy-4-hydroxybenzylidene) cyclohexanone (15a)**. Yellow crystal (yields 35%), mp:155-156°C; ^{1}H NMR (600 MHz, $CDCl_3$) δ 7.79 (s, 1H), 7.77 (s, 1H), 7.48 (dd, J = 10.7, 7.9 Hz, 2H), 7.10 (dd, J = 8.3, 1.7 Hz, 1H), 7.02 (d, J = 1.8 Hz, 1H), 6.98 – 6.94 (m, 3H), 5.88 (s, 1H), 3.95 (s, 3H), 3.87 (s, 3H), 3.02 – 2.91 (m, 5H), 1.88 – 1.78 (m, 2H). ^{13}C NMR (151 MHz, $CDCl_3$) δ 190.19, 159.95, 146.36, 136.90, 136.61, 134.33, 132.25, 128.75, 128.58, 124.43, 114.42, 113.92, 113.25, 55.97, 55.34, 28.54, 23.05. ESI-HRMS: ($C_{28}H_{32}O_6$) calc. [M+H] 351.1518, found 351.1552. **(2*E*,6*E*)-2-(4-methylbenzylidene)-6-(3-methoxy-4-hydroxybenzylidene) cyclohexanone (15c)**. Yellow crystal (yields 55%), mp: 151-153°C; ^{1}H NMR (600 MHz, $CDCl_3$) δ 7.80 (s, 1H), 7.77 (s, 1H), 7.41 (d, J = 8.1 Hz, 2H), 7.24 (d, J = 8.0 Hz, 2H), 7.11 (dd, J = 8.3, 1.8 Hz, 1H), 7.02 (d, J = 1.8 Hz, 1H), 7.01 – 6.96 (m, 1H), 5.86 (s, 1H), 3.95 (s, 3H), 2.96 (td, J = 7.4, 2.0 Hz, 4H), 2.41 (s, 3H), 1.87 – 1.80 (m, 2H). ^{13}C NMR (151 MHz, $CDCl_3$) δ 190.28, 146.45, 146.31, 138.79, 137.12, 136.73, 135.52, 134.29, 133.25, 130.46, 129.14, 128.55, 124.48, 114.42, 113.27, 55.97, 28.61, 28.47, 23.04, 21.41.ESI-HRMS: ($C_{28}H_{32}O_6$) calc. [M+H] 337.1362, found 337.1395. **(b) Representative biological activity procedures.** *Cell Culture*. *Murine macrophages.* The RAW264.7 cells line from the (ATCC® TIB-71™) cells line from the American Type Culture Collection (ATCC) (Manassas, VA, United States) were grown in DMEM containing 10% FBS, 1% (v/v) penicillin G/streptomycin in 5% CO_2 at 37°C. RAW264.7 cells at 80–90% confluency were detached and centrifuged at 1000 RPM in 4°C for 10 min. The cell viability of cultured cells used in the assay was always >95% as determined by trypan blue dye exclusion. *Human macrophages*. U937 (ATCC® CRL 1593.2™) cell line was purchased from American Type Culture Collection (ATCC) (Manassas, VA, United States). U937 mononuclear cell line was grown in the Rosewell Park Memorial Institute-1640 (RPMI-1640) culture media, enriched with 10% (v/v) foetal bovine serum (FBS) and 1% (v/v) penicillin G/streptomycin in 96 wells were maintained at 37°C humidified atmosphere with 5% CO_2. Prior to treatment with the tested compounds, U937 cells (5×10^4 cells/well) were incubated with phorbol 12-myristate 13-acetate (PMA) at concentration 200 nM for 24 hours to allow differentiation from

monocytes to macrophage-like phenotypes. Subsequently, cells were incubated with serum free media overnight for recovery phase. Cell *Stimulation and Treatment*. RAW264.7 and U937 (5×10^5 cells/well) were seeded into a tissue culture grade 96-well plate and incubated for 24 h at 37°C, 5% CO_2 for cell attachment. The attached cells were stimulated in 100 U/mL of recombinant IFN-γ and 2μg/mL of LPS with or without presence of test compound at a final volume of 100μL/well. DMSO was used as vehicle to add test compound into the culture medium and the final concentration of DMSO was 0.1% in all cultures. Cells were then incubated at 37°C, 5% CO_2 for 17–20 h. *Cell Viability*. The cytotoxicity of test compound on cultured cells was determined by assaying the reduction of 3-(4,5-dimethylthiazol-2-yl)-2,5-diphenyltetrazolium bromide (MTT, 5 mg/mL) to formazan salts. After treatment, the supernatant of each wells were removed followed by addition of 20 μL of MTT reagents into each well. The mixture of culture media and MTT were removed after incubated in 37°C for 4 h and the formazan salts were dissolved by adding 100% DMSO. The absorbance was then measured at 570 nm on a SpectraMax Plus microplate reader (Molecular Devices Inc., Sunnyvale, CA, USA) at room temperature. *Determination of PGE_2*. The cell culture supernatants were collected and analyzed for PGE_2 secretion using PGE_2 EIA kits (Cayman Chemical, Ann Arbor, MI, USA). The protocols provided by the manufacturers were followed to the detail. The data was obtained using a SpectraMax Plus microplate reader (Molecular Device, Sunnyvale, CA, USA). The concentration of PGE_2 for each sample was calculated from their respective standard curves. *Cyclooxygenase assay*. The COX-1 and COX-2 inhibition of test compounds were analyzed using COX (ovine/human) inhibitor screening assay kit (Cayman Chemical, Ann Arbor, MI, USA). The protocols provided by the manufacturers were followed to the detail. The data was obtained using a SpectraMax Plus microplate reader (Molecular Device, Sunnyvale, CA, USA). The concentration of PGEs for each sample was calculated from their respective standard curves **(c) X-ray structure determination.** Single crystal X-ray experiment of **15a** and **15c** were performed on Bruker D-QUEST diffractometer using graphite-monochromated Mo-Kα radiation (λ= 0.71073 Å). Intensity data was measured at 301(2) °K by the ω-scan. Accurate cell parameters and orientation matrix were determined by the least-squares fit of 25 reflections. Intensity data was collected for Lorentz and polarization effects. Empirical absorption correction was performed using multiscan. The structure was solved by direct methods and least-squares refinement of the structure was carried out by the SHELXL-97 program. All the non-hydrogen atoms were refined anisotropically. The hydrogen atoms were placed in calculated positions, allowing them to ride on their parent C atom with Uiso(H) = xUeq(C) where, x = 1.5 for methyl; 1.2 for non-methyl groups, except the hydrogen atoms attached to oxygen atoms were located from Fourier maps and refined isotropically. A summary of the data collections and details of the structure refinement is given in Tables 3. Crystallographic data for the structural determination has been deposited with the Cambridge Crystallographic Data Centre, CCDC No **1446853** (**15a**) and **1441911** (**15c**). This information may be obtained free of charge from the Director, CCDC, 12 Union Road, Cambridge CB2, 1EZ, UK;http://www.ccdccam.ac.uk/const/retrieving.html). **(d) Molecular Modeling**. All molecular modeling methods were performed using Discovery Studio 3.1 (Accelrys, San Diego, USA) on an Intel® ™ 2 Quad CPU Q8200 @2.33 GHz running under a Windows XP Professional environment

31. Liew C.Y., Lam K.W., Kim M.K., Harith H.H., Tham C.L., Cheah Y.K., Sulaiman M.R., Lajis N.H., Israf D.A., *Int. Immunopharmacol*., **2011**, *11*, 85.
32. Hosni H.M., Abdulla M.M., *Acta pharmaceutica*, **2008**, *58*, 175.
33. Tran T. D., Park H., Ecker G. F., Thai K. M., *in Proceedings of the 12th International Electronic Conference on Synthetic Organic Chemistry* (ECSOC '08), **2008**
34. Chanput W., Peters V., Wichers H., Verhoeckx K., Cotter P., López-Expósito I., Kleiveland C., Lea T., Mackie A., Requena T., Swiatecka D., Wichers H. (Eds.), *Springer International Publishing*, **2015**, pp. 147-159.
35. Pawelzik S.C., Uda N.R., Spahiu L., Jegerschold C., Stenberg P., Hebert H., Morgenstern R., Jakobsson P.J., *J Biol Chem*, **2010**, *285*, 29254.
36. Tham C.L., Hazeera Harith H., Wai Lam K., Joong Chong Y., Singh Cheema M., Roslan Sulaiman M., Lajis N.H., Israf D.A., *Eur. J. Pharmacol.*, **2015**, 749, 1.
37. Amaravani M., Prasad N., Ramakrishna V., *SpringerPlus*, **2012**, *1*, 58.
38. Pan Y., Zhang X., Wang Y., Cai L., Ren L., Tang L., Wang J., Zhao Y., Wang Y., Liu Q., Li X., Liang G., *PLoS ONE*, **2013**, *8*, 79084.
39. Zhu S., Moore T.W., Lin X., Morii N., Mancini A., Howard R.B., Culver D., Arrendale R.F., Reddy P., Evers T.J., Zhang H., Sica G., Chen Z.G., Sun A., Fu H., Khuri F.R., Shin D.M., Snyder J.P., Shoji M., *Integr. Biol.*, **2012**, *4*, 633.
40. Thomas S.L., Zhao J., Li Z., Lou B., Du Y., Purcell J., Snyder J.P., Khuri F.R., Liotta D., Fu H., *Biochem. Pharmacol*., **2010**, *80*, 1309.
41. Plummer S.M., Holloway K.A., Manson M.M., Munks R.J., Kaptein A., Farrow S., Howells L., *Oncogene*, **1999**, *18*, 6013.
42. Moore T.W., Zhu S., Randolph R., Shoji M., Snyder J.P., *Med. Chem. Lett.*, **2014**, *5*, 288.